USING VORTICITY FLUX TO CHARACTERIZE A BOUNDARY LAYER

David Nixon
Consultant
Los Altos; California; USA

Abstract
A set of equations that represent the gross features of a boundary layer are derived from the vorticity flux equations. Other than the classic eddy viscosity representation of turbulence, there are no approximations in the derivation. Flow separation, transition and other flow phenomena can be represented explicitly in terms of flow quantities that can be controlled. In particular, the concept of added turbulence as a control is exploited for a range of flow separation problems.

Introduction
Boundary layer theory was developed by Prandtl (1) over 100 years ago and has proved an essential tool in predicting the flow around aircraft as well as providing a framework for analyzing flow details. In the last few decades computational fluid dynamics (CFD) has largely replaced the boundary layer model as part of an aerodynamic prediction method but its theoretical picture of aerodynamics is still used as a framework for analyzing air flows. In this paper an alternative to the classic boundary layer model is proposed that enables a different framework for analyzing flow separation and other viscous dominated problems. The research is motivated by the idea that aerodynamics science might be advanced if outstanding problems are re-examined from a non-traditional perspective.

The present research uses the vorticity flux equations to derive equations that represent most of the gross features of a boundary layer, including separation and transition. These equations relate flow characteristics that *need* to be controlled to factors that *can* be controlled. Other than the Boussinesq (2) relation for representing turbulence, no approximations are used in the derivation.

Since no approximations are used in their derivation these "new" boundary layer equations should represent all of the flow conditions commonly associated with boundary layers. The representation of separation, transition, buffet and aerodynamic lift is described in the paper. Some flow control strategies are also described in the context of the boundary layer equations.

Examples and Computations
Although the basic equations are derived for three dimensional flow, only two dimensional examples are considered for reasons of simplicity in presentation. The ideas developed in the research were tested using a CFD code to solve the Navier-Stokes equations. This code is a variation of that described in Ref. [3] and includes the Baldwin-Lomax (4) and Spalart-Allmaras (5) turbulence models.

Analysis
In the following analysis (x, y, z) are Cartesian coordinates, fixed in space, with velocity components (u, v, w); the total velocity is "q" and C_p is the pressure coefficient. ρ denotes the density and $\bar{t}$ is the time. All variables are scaled with respect to their freestream values, denoted by the subscript ∞.

The momentum equations in the Reynolds averaged Navier Stokes equations (see, for example Ref. [6]) can be re-written in Cartesian coordinates, (x, y, z) as follows

$$\rho\frac{\partial u}{\partial \bar{t}} - \rho v\Omega_3 + \rho w\Omega_2 + \rho\frac{1}{2}\frac{\partial q^2}{\partial x} = -\frac{1}{2}\frac{\partial C_p}{\partial x} + S_x \qquad [1a]$$

$$\rho\frac{\partial v}{\partial \bar{t}}-\rho w\Omega_1+\rho u\Omega_3+\rho\frac{1}{2}\frac{\partial q^2}{\partial y}=-\frac{1}{2}\frac{\partial c_p}{\partial y}+S_y \qquad [1b]$$

$$\rho\frac{\partial w}{\partial \bar{t}}-\rho u\Omega_2+\rho v\Omega_1+\rho\frac{1}{2}\frac{\partial q^2}{\partial z}=-\frac{1}{2}\frac{\partial c_p}{\partial z}+S_z \qquad [1c]$$

In Eq. [1] the S_x, S_y, S_z terms on the right hand side are the viscous stress terms. Note that if the Boussinesq (2) approximation is used the coefficient of viscosity includes an eddy viscosity component that represents turbulence. Ω_1, Ω_2 and Ω_3 denote the vorticity components in the (x,y,z) directions respectively and are defined by

$$\Omega_1=\frac{\partial w}{\partial y}-\frac{\partial v}{\partial z}:\ \Omega_2=\frac{\partial u}{\partial z}-\frac{\partial w}{\partial x}:\ \ \Omega_3=\frac{\partial v}{\partial x}-\frac{\partial u}{\partial y} \qquad [2]$$

In a generalized body fitted curvilinear coordinate system, (ξ,η,ζ,τ), where

$$\xi=\xi(x,y,z,\bar{t}):\ \ \eta=\eta(x,y,z,\bar{t}):\ \ \zeta=\zeta(x,y,z,\bar{t}):\ \ \tau=\bar{t} \qquad [3]$$

and ($\zeta=0$) represents the body surface, Eqs. [1] can be combined to give

$$\frac{\rho}{J}(a_1u_\tau+a_2v_\tau+a_3w_\tau)+\frac{\rho}{J}Q_{11}+\frac{\rho}{J}Q_{12}+\frac{\rho}{J}Q_{13}+\frac{\rho\tilde{w}}{J}\bar{\Omega}_2-\frac{\rho\tilde{v}}{J}\bar{\Omega}_3$$
$$=\frac{1}{2}\frac{\partial\bar{c}_p}{\partial\xi}+\frac{q^2}{2}\frac{\partial\rho}{\partial\xi}+\frac{1}{J}(a_1S_x+a_2S_y+a_3S_z) \qquad [4a]$$

$$\frac{\rho}{J}(b_1u_\tau+b_2v_\tau+b_3w_\tau)+\frac{\rho}{J}Q_{21}+\frac{\rho}{J}Q_{22}+\frac{\rho}{J}Q_{23}+\frac{\rho\tilde{u}}{J}\bar{\Omega}_3-\frac{\rho\tilde{w}}{J}\bar{\Omega}_1$$
$$=\frac{1}{2}\frac{\partial\bar{c}_p}{\partial\eta}+\frac{q^2}{2}\frac{\partial\rho}{\partial\eta}+\frac{1}{J}(b_1S_x+b_2S_y+b_3S_z) \qquad [4b]$$

$$\frac{\rho}{J}(c_1u_\tau+c_2v_\tau+c_3w_\tau)+\frac{\rho}{J}Q_{31}+\frac{\rho}{J}Q_{32}+\frac{\rho}{J}Q_{33}+\frac{\rho\tilde{v}}{J}\bar{\Omega}_1-\frac{\rho\tilde{u}}{J}\bar{\Omega}_2$$
$$=\frac{1}{2}\frac{\partial\bar{c}_p}{\partial\zeta}+\frac{q^2}{2}\frac{\partial\rho}{\partial\zeta}+\frac{1}{J}(c_1S_x+c_2S_y+c_3S_z) \qquad [4c]$$

In Eq. [4]

$$J=\begin{vmatrix}\xi_x&\xi_y&\xi_z\\ \eta_x&\eta_y&\eta_z\\ \zeta_x&\zeta_y&\zeta_z\end{vmatrix}:\qquad \begin{pmatrix}a_1&b_1&c_1\\ a_2&b_2&c_2\\ a_3&b_3&c_3\end{pmatrix}=J\begin{pmatrix}\xi_x&\xi_y&\xi_z\\ \eta_x&\eta_y&\eta_z\\ \zeta_x&\zeta_y&\zeta_z\end{pmatrix}^{-1} \qquad [5]$$

The terms, Q_{11}, Q_{12}, Q_{13} etc. are defined by

$$\begin{pmatrix}Q_{11}&Q_{21}&Q_{31}\\ Q_{12}&Q_{22}&Q_{32}\\ Q_{13}&Q_{23}&Q_{33}\end{pmatrix}=\begin{pmatrix}\xi_{\bar{t}}a_1&\xi_{\bar{t}}a_2&\xi_{\bar{t}}a_3\\ \eta_{\bar{t}}b_1&\eta_{\bar{t}}b_2&\eta_{\bar{t}}b_3\\ \zeta_{\bar{t}}c_1&\zeta_{\bar{t}}c_2&\zeta_{\bar{t}}c_3\end{pmatrix}\begin{pmatrix}u_\xi&u_\eta&u_\zeta\\ v_\xi&v_\eta&v_\zeta\\ w_\xi&w_\eta&w_\zeta\end{pmatrix} \qquad [6]$$

and

$$\overline{c}_p = 1 - c_p - \rho q^2 \qquad [7]$$

The remaining terms in Eq. [4] are

$$\tilde{u} = \xi_{\bar{t}} + \xi_x u + \xi_y v + \xi_z w:\ \tilde{v} = \eta_{\bar{t}} + \eta_x u + \eta_y v + \eta_z w:\ \tilde{w} = \zeta_{\bar{t}} + \zeta_x u + \zeta_y v + \zeta_z w \qquad [8]$$

and

$$\overline{\Omega}_1 = \xi_x \Omega_1 + \xi_y \Omega_2 + \xi_z \Omega_3:\ \overline{\Omega}_2 = \eta_x \Omega_1 + \eta_y \Omega_2 + \eta_z \Omega_3:\ \overline{\Omega}_3 = \zeta_x \Omega_1 + \zeta_y \Omega_2 + \zeta_z \Omega_3 \qquad [9]$$

Definition of a "Boundary Layer"

In a subsonic, wall bounded, flow the only sources of vorticity are the viscous stresses generated by the interaction of the flowing fluid and the wall. This vorticity is often confined to a region close to the wall and a physically plausible definition of a "boundary layer" is the region where the vorticity magnitude exceeds a small value: it need not be thin as in classic theory. Because there are three components of vorticity it is possible to define three different boundary layer edges. In the present analysis the boundary layer is defined as the region in which

$$\max\left(|\Omega_1|, |\Omega_2|, |\Omega_3|\right) \succ \varepsilon: \qquad \varepsilon = 10 \qquad [10]$$

In Eq. [8] $\tilde{w}$ is the velocity component normal to the wall and is zero at the wall by the "no-slip" boundary condition. If $\tilde{w}$ remains small throughout the boundary layer, which implies that the flow is nearly parallel to the wall in the boundary layer, then the product of $\tilde{w}$ and any vorticity component will be small. Thus the degree of normal vorticity flux in the boundary layer can be defined as either $\int_0^\delta \frac{\rho\tilde{w}}{J}\overline{\Omega}_2 d\zeta$, $\int_0^\delta \frac{\rho\tilde{w}}{J}\overline{\Omega}_1 d\zeta$ or $\int_0^\delta \frac{\rho\tilde{w}}{J}\overline{\Omega}_3 d\zeta$, where δ is the boundary beyond which vorticity is negligible (that is, the "boundary layer" edge). Expressions for the first two of these integrals can be constructed by integrating Eq. [4a] and Eq. [4b] respectively. These can be rearranged as

$$\int_0^\delta \frac{\rho\tilde{w}}{J}\overline{\Omega}_2 d\zeta = \int_0^\delta \frac{\rho\tilde{v}}{J}\overline{\Omega}_3 d\zeta + \frac{1}{2}\int_0^\delta \frac{\partial \overline{c}_p}{\partial \xi} d\zeta + \int_0^\delta \frac{q^2}{2}\frac{\partial \rho}{\partial \xi} d\zeta - \int_0^\delta \frac{\rho}{J}\left(a_1 u_\tau + a_2 v_\tau + a_3 w_\tau\right) d\zeta$$
$$- \int_0^\delta \left(\frac{\rho}{J}Q_{11} + \frac{\rho}{J}Q_{12} + \frac{\rho}{J}Q_{13}\right) d\zeta + \int_0^\delta \frac{1}{J}\left(a_1 S_x + a_2 S_y + a_3 S_z\right) d\zeta \qquad [11a]$$

$$\int_0^\delta \frac{\rho\tilde{w}}{J}\overline{\Omega}_1 d\zeta = \int_0^\delta \frac{\rho\tilde{u}}{J}\overline{\Omega}_3 d\zeta - \frac{1}{2}\int_0^\delta \frac{\partial \overline{c}_p}{\partial \eta} d\zeta - \int_0^\delta \frac{q^2}{2}\frac{\partial \rho}{\partial \eta} d\zeta + \int_0^\delta \frac{\rho}{J}\left(b_1 u_\tau + b_2 v_\tau + b_3 w_\tau\right) d\zeta$$
$$+ \int_0^\delta \left(\frac{\rho}{J}Q_{21} + \frac{\rho}{J}Q_{22} + \frac{\rho}{J}Q_{23}\right) d\zeta - \int_0^\delta \frac{1}{J}\left(b_1 S_x + b_2 S_y + b_3 S_z\right) d\zeta \qquad [11b]$$

A third equation for $\int_0^\delta \frac{\rho\tilde{u}}{J}\overline{\Omega}_2 d\zeta$ can be derived from Eq. [4c], namely

$$\int_0^\delta \frac{\rho\tilde{u}}{J}\overline{\Omega}_2 d\zeta = \int_0^\delta \frac{\rho\tilde{v}}{J}\overline{\Omega}_1 d\zeta + \frac{1}{2}\left[\overline{c}_p(\delta) - \overline{c}_p(0)\right] - \int_0^\delta \frac{\rho}{J}\left(c_1 u_\tau + c_2 v_\tau + c_3 w_\tau\right) d\zeta$$
$$- \int_0^\delta \left(\frac{\rho}{J}Q_{31} + \frac{\rho}{J}Q_{32} + \frac{\rho}{J}Q_{33}\right) d\zeta + \int_0^\delta \frac{1}{J}\left(c_1 S_x + c_2 S_y + c_3 S_z\right) d\zeta + \int_0^\delta \frac{q^2}{2}\frac{\partial \rho}{\partial \zeta} d\zeta \qquad [11c]$$

Eq. [11] are the basic boundary layer equations. There are no approximations other than those inherent in the Navier-Stokes equations that use the Boussinesq [2] approximation for turbulence. The degree of turbulence is represented by the eddy viscosity.

Representation of Flow Conditions

Separation

The integral of the normal vorticity flux for a two dimensional flow around an airfoil at different angles of attack is shown in Fig. [1]. The test case is the flow around a NACA0012 airfoil section at a freestream Mach number of 0.3 at a Reynolds number of six million. The stall status of each flow (defined by a maximum in the lift curve) is shown in the legend. It can be seen that stall can be identified by the integral of the normal vorticity flux. It is suggested that stall occurs when the integral of the normal vorticity flux becomes a significant positive value. Thus stall does not occur for $\xi_{LE} \le \xi \le \xi_{TE}$ if

$$\int_0^{\delta} \frac{\rho}{J} \tilde{w} \overline{\Omega}_2 d\zeta \prec \varepsilon \qquad [12a]$$

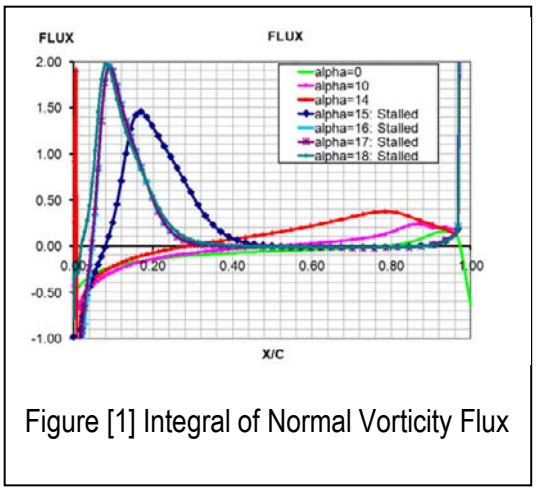

Figure [1] Integral of Normal Vorticity Flux

where ε is a small positive number. For a three dimensional flow there is an additional condition, namely that

$$\int_0^{\delta} \frac{\rho}{J} \tilde{w} \overline{\Omega}_1 d\zeta \prec \varepsilon \qquad [12b]$$

for $\xi_{LE} \le \xi \le \xi_{TE}$ must also be satisfied. In most cases $\left|\overline{\Omega}_1\right| \prec\prec \left|\overline{\Omega}_2\right|$ and Eq. [12a] will be the critical condition. A composite version of Eq. [12a] and Eq. [12b] is

$$\int_0^{\delta} \frac{\rho}{J} \tilde{w} \sqrt{\overline{\Omega}_1^2 + \overline{\Omega}_2^2} d\zeta \prec \varepsilon \qquad [12c]$$

Positive values of the integral of normal vorticity flux indicate flow "separation". If the flow is separated completely, as it is for the aft part of the airfoil, then the integral of normal vorticity flux is again close to zero. This implies that a significant positive value of the integral of normal vorticity flux means not just that the flow is separated in that region but may imply that the flow aft of the region is also separated. The negative value of flux near the leading edge is due to the high curvature of the particle paths, which adds a significant gradient to $\bar{w}$.

Measure of Separation

This definition of separation suggests that a measure of "separation" is the chordwise integral of the positive portion of the flux integral. Thus the parameter that measures the extent of the separation is

$$I_f = \int_0^1 \int_0^{\delta} \left[\frac{\rho}{J} \tilde{w} \overline{\Omega}_2 \right]_{positive} d\zeta d\xi \qquad [13]$$

The integral in Eq. [13] is called the separation integral.

Transition

Eq. [11a] can be written as

$$I_{w2} = I_{v3} + I_{cp} + I_{\rho} - I_{\tau}(\tau) + I_{Q} + I_{\sigma}(\nu) \qquad [14]$$

where the terms represent, in order, the integrals in Eq. [11a]. Eq. [11b] and Eq. [11c] can be written in similar form. If the airfoil does not move then, in Eq. [14], $I_{Q} = 0$.

If the airflow is steady then

$$I_{\tau}(\tau) = 0 \qquad [15]$$

If the flow is laminar then

$$I_{\sigma}(\hat{\nu}) = 0 \qquad [16]$$

where $\hat{\nu}$ is the coefficient of kinematic eddy viscosity.

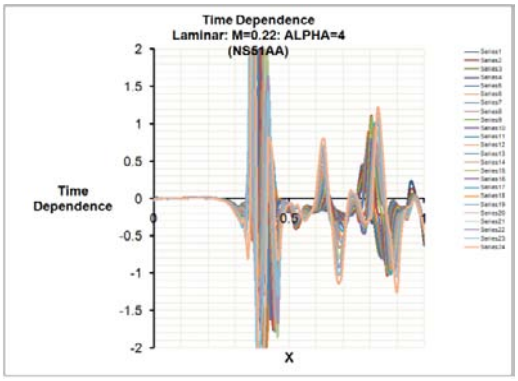

Figure [2] Time Dependence Integral: Laminar: (30,000 time steps)

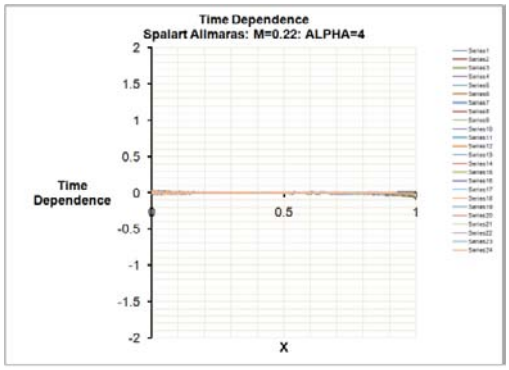

Figure [3] Time Dependence Integral: Turbulent: (30,000 time steps)

If the flow is initially laminar and steady but then becomes unsteady so that

$$I_{\tau}(\tau) \neq 0 \qquad [17]$$

then it is plausible that this unsteadiness can be countered by the introduction of turbulence that changes the eddy viscosity component of ν and hence $I_{\sigma}(\nu)$. In other words two solutions can exist, one laminar and unsteady and the other steady and turbulent. This model implies that the large scale unsteadiness associated with the laminar flow can be transferred to the small scale unsteadiness associated with turbulent flow. The turbulent flow can then be represented by an eddy viscosity.

Alpha	X_{TR} Present	X_{TR} Experiment
0	0.405	0.416
2	0.349	0.355
4	0.319	0.288
6	0.228	0.224

Predicted and Experimental Transition Points: Subsonic Flow
Table 1

An example of such an unsteady laminar flow is illustrated in Fig. [2]. The airfoil is the NLF (2) 416 section at a Mach number of 0.22 and a Reynolds number of 5 million. The angle of attack is 4 deg. A grid of 496 x 88 is used and the computation was run for 30,000 time steps. The chordwise variation of the integral $I_{\tau}(\tau)$ for the last 4800 time steps, at 200 step intervals, is shown. It can be seen that the integral becomes very large over the rear part of the airfoil. In effect there is a limit cycle. In contrast, the same calculation for turbulent flow, using the Spalart-Allmaras [5] turbulence model, gives an almost zero value for $I_{\tau}(\tau)$ (see Fig. [3]). This suggests that when $I_{\tau}(\tau) = 0$ the flow can be laminar but when this condition is not met then the flow can be turbulent with the (steady) turbulence term $I_{\sigma}(\nu)$ now absorbing the effect of a non-zero $I_{\tau}(\tau)$. The start of the turbulence generation is the point when $I_{\tau}(\tau)$ ceases to be zero.

Boundary layer transition is assumed to occur at the point, $x = x_{tr}$, before which Eq. [15] is satisfied. Using Eq. [15] to predict transition onset, a series of computations for the NLF (2) 416 airfoil at different angles of attack were performed. The results for the transition station, X_{TR}, are compared to experimental data [7] in Table 1. The agreement is surprisingly good. The transition limit cycle is linked to an unsteady flow separation.

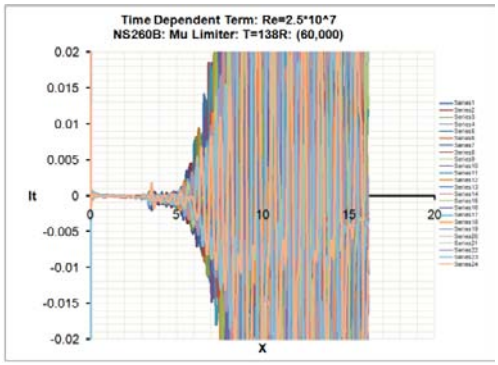

Figure [4] I_τ for Blunted Cone: $\mathrm{Re}\big|_{RN} = 960,000$: M=6

The integral across the boundary layer thickness of the kinetic energy generated by the laminar limit cycle was computed. The energy represented by the turbulence was also integrated across the boundary layer. Interestingly, there is a correspondence in energy close to the transition point, which might indicate that a transfer from laminar to turbulent flow at constant energy is possible at this point. However, the energy *distribution* over the boundary layer may not be the same for turbulence and the laminar limit cycle.

This definition of transition is applied to the hypersonic flow over a spherically blunted cone at M=6.0 (see Fig. [4]). The Reynolds' number based on the nose radius is 9.6×10^5. The computations are continued for a minimum of 60,000 time steps. The characteristic limit cycle for transition is apparent. However, the predicted transition point is much further aft ($\approx$143 nose radii) than the experimental value found by Stetson (see Ref. [8]) of around 53 nose radii. This may be due to the fact that the computation is axi-symmetric, ruling out transverse disturbances or because of the use of numerical limiters on flow unsteadiness at the nose.

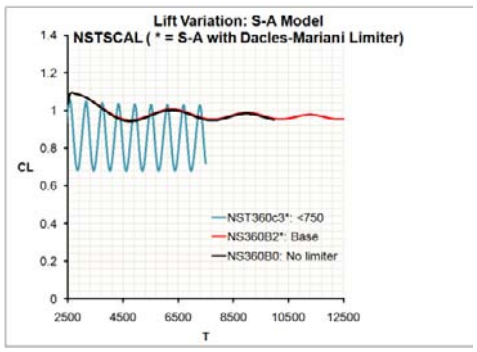

Figure [5] Buffet as a Consequence of Limiting Eddy Viscosity

The general idea of these transition calculations is that, since the Navier Stokes equations represent all instabilities, a direct computation identifies those that *grow to a limit cycle* as opposed to the commonly used stability equations that identify all growing instabilities. There has been no attempt to introduce explicit instability waves into the computations.

Buffet

In a similar way as transition, buffet will occur if the production of turbulence (a damping influence) is insufficient to eliminate flow instabilities, resulting in an unsteady flow limit cycle. This assertion is indicated by the research of Alfano [9] in which it is noted that turbulence (actually eddy viscosity) must be limited to compute the experimentally observed limit cycles caused by shock induced separation. It is also indicated by attempts to simulate transonic buffet which required a limit on the eddy viscosity in order to be successful (see Fig. [5]). In the latter case the airfoil is the NASA SC-(2) 714 section at 3.25 deg angle of attack, the Reynolds' number is 1.5×10^7, $M_\infty = 0.725$. This is close to one of the cases reported by Bartels [10]. The Spalart-Allmaras turbulence model [5] is used. The base solution gives almost a steady flow. A limiter on the value of the eddy viscosity is then imposed (<750) and this does give a limit cycle. The limiter really only affects the eddy viscosity behind the shock wave. Note that the frequency of the oscillatory solution is an order of magnitude lower than the expected (experimental)

value. The reasons for this discrepancy are unclear but it does not alter the conclusion that buffet occurs when the eddy viscosity, and consequently turbulence, is limited.

Aerodynamic Lift

Eq. [11c] can be written as

$$I_{u2} = -\frac{1}{2}\overline{C}_p(0) + I_{\rho\xi} - I_{\tau\xi}(t) + I_{Q\xi} + I_{\sigma\xi}(\nu) \qquad [18]$$

where the terms represent, in order, the integrals in Eq. [11c]. Also, the upper limit of integration is taken to be $\zeta = \infty$ where it is assumed that $\lim_{\zeta\to\infty}\overline{C}_p(\zeta) \to 0$. Eq. [18] can be re-arranged to give

$$\frac{1}{2}C_p(0) = I_{u2} - I_{\rho\xi} + I_{\tau\xi} - I_{Q\xi} - I_{\sigma\xi} - \frac{1}{2}\rho q^2\Big|_{\zeta=0} \qquad [19]$$

Note that "q" is not zero on a moving surface and is dependent on the motion.

Eq. [19] can be used to construct the following relation.

$$\frac{1}{2}\Delta C_p(0) = -\Delta I_{u2} + \Delta I_{\rho\xi} - \Delta I_{\tau\xi} + \Delta I_{Q\xi} + \Delta I_{\sigma\xi} + \frac{1}{2}\Delta\left(\rho q^2\right)\Big|_{\zeta=0} \qquad [20]$$

where "Δ" denotes the difference between values in the upper and lower half planes.

The pressure difference can then be integrated along the chord to give the normal force.

$$\frac{1}{2}C_N = -\int_0^c \Delta I_{u2}\bar{n}d\xi + \int_0^c \Delta I_{Q\xi}\bar{n}d\xi + \int_0^c \Delta I_{\sigma\xi}\bar{n}d\xi + \int_0^c \Delta I_{\rho\xi}\bar{n}d\xi - \int_0^c \bar{n}\Delta I_{\tau\xi}d\xi + \frac{1}{2}\int_0^c \Delta\left(\rho q^2\right)\Big|_{\zeta=0}\bar{n}d\xi \qquad [21]$$

where $\bar{n}$ is the normal of the surface element "dξ" to the airfoil chord line. Eq. [21] shows the relationship between normal force, the streamwise vorticity flux, the viscous stresses and motion.

The time dependent terms in Eq. [21] are nonlinear which suggests that the normal force averaged over a periodic cycle is dependent on the root mean square of the motion. Eq. [21] may also provide clues as to the nature of flapping flight. Since the equation also shows the Reynolds number dependence through $I_{\sigma\xi}$ it should also provide insight into the nature of lift in low Reynolds number flight.

Eq. [20] indicates that control of $\Delta I_{\tau\xi}$ (and the surface velocities) (perhaps with boundary layer blowing or a very high frequency, very low amplitude surface deformation) can control the local pressure coefficient. Note that it is possible to get large magnitudes of $\Delta I_{\tau\xi}$ and the surface velocities without large surface deformations if the frequency is sufficiently large.

Flow Control

Eq. [14] relates flow characteristics that *need to be controlled,* such as I_{w2} (separation) or $I_\tau(t)$ (transition) to those that *might be controllable*, such as I_σ (added turbulence) or I_Q (dynamic geometry changes) as well as the obvious stationary geometry changes represented by the transformation metrics. Note that separation can be controlled directly by suction, which alters $\tilde{w}$.

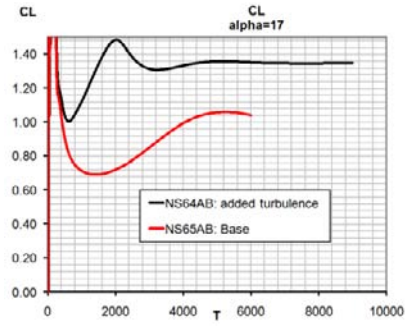

Figure [6] Temporal Behavior of Lift: alpha=17 deg

In the examples given here the idea of added turbulence is used. Added turbulence changes the eddy viscosity in I_σ and may be implemented physically by a Gurney flap or by some mechanism that provides the same amount of extra turbulence but less pressure drag. The actual mechanism is not considered here. Generally the extra turbulence is inserted in the outer part of the boundary layer. The importance of the outer part of the boundary layer may be explained as follows. I_{w2} is written as

$$\int_0^{\delta} \frac{\rho}{J}\tilde{w}\boldsymbol{\Omega}_2 d\zeta = \int_0^{\bar{\delta}} \frac{\rho}{J}\tilde{w}\boldsymbol{\Omega}_2 d\zeta + \int_{\bar{\delta}}^{\delta} \frac{\rho}{J}\tilde{w}\boldsymbol{\Omega}_2 d\zeta \qquad [22]$$

where $\bar{\delta}$ is the outer limit of the region in which $\tilde{w} \approx 0$. This implies that the first integral in Eq. [22] is small and does not contribute to I_f . By simply replacing δ by $\bar{\delta}$ it then follows from Eq. [11a] that

$$\frac{1}{2}\frac{\partial}{\partial \xi}\int_0^{\bar{\delta}}\left[\bar{c}_p(\zeta)\right]d\zeta - \int_0^{\bar{\delta}}\frac{\rho}{J}\left(\xi_x u_\tau + \xi_z w_\tau\right)d\zeta - \dot{\alpha}\int_0^{\bar{\delta}}\frac{\rho}{J}Q d\zeta + \int_0^{\bar{\delta}} S_w d\zeta \approx 0 \qquad [23]$$

Eq. [23] implies that the critical part of Eq. [11] is for $\zeta \succ \bar{\delta}$. The added eddy turbulence is a similar order of magnitude as wake turbulence behind a Gurney flap. The extent of the turbulence 'source", in the normal direction, is about 1% -1.5% of chord, indicating that a similar level of turbulence could be produced by a Gurney flap of similar size.

Steady Stall

The test case is a NACA0012 airfoil section at a freestream Mach number of 0.3 and a Reynolds number of six million. The Spalart-Allmaras [5] turbulence model is used. The effect of added turbulence on the lift at 17 deg angle of attack is shown in Fig. [6]. The effect is considerable. The energy of the added turbulence is associated with a drag; for this case the additional drag coefficient is very small, namely 0.000118.

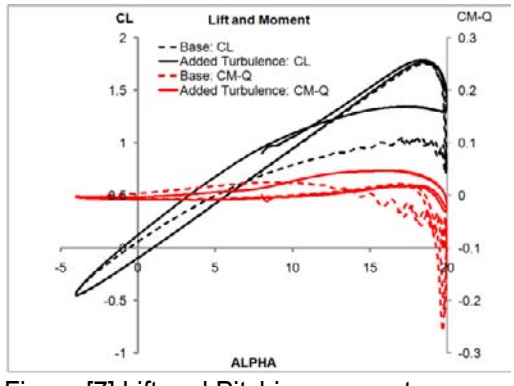

Figure [7] Lift and Pitching moment Coefficients for Dynamic Stall

Dynamic Stall

The test case is a NACA0012 airfoil section at a freestream Mach number of 0.3 and a Reynolds number of one million. The mean angle of attack is 8 deg and the airfoil is oscillating in a sinusoidal motion with an amplitude of 12 deg. The reduced frequency, based on chord, is 0.025. The Baldwin-Lomax [4] turbulence model is used. Turbulence is added when the magnitude of the pitching moment about the quarter chord exceeds 0.025. The effect of added turbulence on the lift and pitching moment (about 25% chord) coefficients is shown in Fig. [7]. The added turbulence reduces the characteristic drop in lift considerably and virtually eliminates the pitching moment overshoot that is a critical factor in helicopter rotor design. A similar result can be attained by changing the motion to be non-sinusoidal; that is, altering I_Q in Eq. [14].

Shock Induced Separation

The test case is a NACA0012 airfoil section at a freestream Mach number of 0.8, a Reynolds number of three million and angle of attack of 3 deg. The Spalart-Allmaras [5] turbulence model is used. The extra turbulence is added only in the region of the shock foot where the "vorticity shock" [11] is located; the added turbulence region extends over about 18% chord. The change in pressure distribution due to added turbulence is shown in Fig. [8].The added turbulence reduces the magnitude of the separation integral by about 30% and the lift/drag ratio is increased by over 6%.

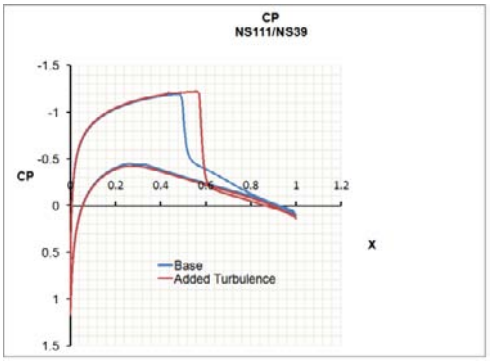

Figure [8] Effect of Added Turbulence on Shock Induced Separation

Future Research

The main topic of this paper is the derivation of the equations for the integrals of the vorticity flux. These equations give a different, and unified, insight into flow separation, transition to turbulence, buffet and aerodynamic lift. The equations should be studied in much more detail, and exploited, especially the three dimensional aspects and the nature of the limit cycles that arise at the onset of turbulence and in buffet. The analysis of buffet suggests that the maximum net production of turbulence plays a critical part and therefore the reasons why turbulence ceases to grow need to be identified and possible control strategies formulated. Note that turbulence can be regarded as a form of limit cycle in that *on average* it is an unsteady motion that does not grow or decay.

There are two important flow control topics that require much further research. The first is the idea of added viscosity (or turbulence) to control flow separation; the second is the opportunity to directly incorporate a measure of flow separation (the separation integral) into an optimizer.

Some Specific Topics

The research described here looks at the two dimensional version of the vorticity flux equations, mainly because much greater computer resources are required to help investigate three dimensional problems. Studies of transition would benefit greatly from the availability of increased computing power. Also, for three dimensional flows there are two vorticity flux equations that must be closely examined to find new physical concepts.

Turbulence modeling is also important especially for studies of buffet. Since it is suggested that the cause of buffet is an inability of the flow to create sufficient turbulence to damp an incipient limit cycle, further knowledge of a physical turbulence maximum is needed. Although there are turbulence models with "realizablity constraints" these constraints are more to do with limiting spurious turbulence production in the model rather than the physics of a turbulence limit.

The ominous presence of limit cycles in transition and buffet is striking. The driving force behind these limit cycles is not known. It is suggested in Ref. [12] that any phenomenon that depends on, and lags, the outer "inviscid" flow can create a limit cycle. This suggestion should be studied in much greater depth if buffet and transition are to be understood.

In most of the applications the added viscosity is "inserted" in the outer part of the boundary layer. It is not easy to see how this could be done physically without causing structural complications. The only "easy to install" devices that are identified are a slat, in which the slat wake gives the added turbulence, and a Gurney flap. Because of the importance of added turbulence this might suggest that the slat trailing edge should be blunt (to increase turbulence in its wake) and that the Gurney "flap" should be

more bullet shaped to reduce pressure drag. In general, the invention of any device that can introduce turbulence in the outer part of the boundary layer would be beneficial. These flow control strategies apply to a reduction of the adverse effects of the vorticity shock (11) as well as other flow separation events.

Since the vorticity flux equations (and the "separation integral") provide a well defined objective function for optimization an obvious research strategy is to couple an optimizer with a CFD code to investigate how best to control flow separation or transition. This has not really been addressed here (apart from the simple dynamic stall case) because of the unavailability of sufficient computer power.

References

1. Prandtl, L. "Ueber Flussigkeitsbewegung bei sehr kleiner Reibung", Proc. 3rd Int. Math. Congress, Heidelburg, 1904
2. Boussinesq, J. "Theorie de l'ecoulement tourbillant", Mem. Pres. Acad. Sci. Paris, Vol 23, page 46, 1877
3. Srinivasan, G.R. & Baeder, J.D. "TURNS: A Free-Wake Euler/Navier-Stokes Numerical Method for Helicopter Rotors" AIAA Journal Vol. 31, No. 5 1993
4. Baldwin, B. S. & Lomax, H. "Thin Layer Approximation and Algebraic Model for Separated Turbulent Flow", AIAA Paper, 78-0257, 1978
5. Spalart, P.R & Allmaras, S.R. "A One Equation Turbulence Model for Aerodynamic Flows" AIAA Paper 92-0439, 1992
6. Anderson, D. et al "Computational Fluid Mechanics and Heat Transfer", Hemisphere, 1984
7. Krishnan, V. et al "Transition-Related Studies on Two Low Drag Airfoils", Current Science, Vol. 79, No 6, 2000
8. Schneider, S. P. "Hypersonic Laminar-Turbulent Transition on Circular Cones and Scramjet Fore-bodies" Prog. Aero. Sci, Vol. 40, 2004
9. Alfano, D. et al "Numerical Simulation of Shock/Boundary Layer Self Sustained Oscillations for External and Internal Flows", AIAA Paper 2006-2840, 2006
10. Bartels, R. E. "Flow and Turbulence Modeling and Computation of Shock Buffet Onset for Conventional and Supercritical Airfoils", NASA TP-1998-206908, 1998
11. Nixon, D. "Shock Waves, Vorticity and Vorticity Shocks", AIAA Paper 2007-1287, 2007
12. Nixon, D. "Macro-Aerodynamics:-A Phenomenological Model of Highly Non-Linear Aerodynamics", SAE Paper 2002-01-2913, 2002

Contact: David Nixon: davidnixon@sbcglobal.net